Multiscale and Multidisciplinary Modeling, Experiments and Design
https://doi.org/10.1007/s41939-024-00568-3

ORIGINAL PAPER

Mechanical, microstructural, and durability assessment of ambient cured geopolymer concrete

Auxilia Rani A[1] · **Sudha C**[1]

Received: 12 July 2024 / Accepted: 6 August 2024

Abstract
This research conducted a thorough analysis of the properties of geopolymer concrete material, utilizing fly ash and ground granulated blast furnace slag as the primary components. The activation of this precursor was achieved by using an alkaline solution composed of sodium hydroxide and sodium silicate. The mix design formulation adhered to the specifications outlined in the IS code and several tests were conducted to attain the most advantageous result. Afterwards, the mechanical characteristics and microstructure of the best combination were evaluated using typical curing conditions, including a brief assessment of its durability. The results indicate that the geopolymer concrete, composed of 60% fly ash and 40% ground granulated blast furnace slag, achieved its highest compressive strength after 28 days with a 2–5% rise in strength between days 28 and 56. The microstructure study demonstrated a clear and precisely organized polymeric structure. The durability investigation revealed that the material is moderately vulnerable to acidic environments, different sulfate reactions, and increased compression resistance in chloride-rich settings. Additionally, the material maintains good levels of water absorption around 4.86%, and a balanced porosity level of approximately 9.73% permeable voids. By utilizing Response Surface Methodology (RSM), it became possible to analyze the optimum compressive strength. As a result, a robust model was created, demonstrating a high level of reliability, with an R^2 value of 0.98. The innovative aspect of this work is the self-designed mix that was created and improved over several experiments to find the ideal ratio of 40–60% GGBS, which improved the mix's mechanical properties and durability. The study emphasizes the importance of improving mix designs to improve geopolymer concrete's mechanical qualities, durability, and environmental sustainability.

Keywords Geopolymer concrete · Fly ash · Ground granulated blast furnace slag · Alkaline activation · Compressive strength · Durability

1 Introduction

The utilization of geopolymer concrete in buildings has been growing due to its eco-friendly qualities and sustainability, particularly its long lifespan and reduced carbon emissions. Ordinary Portland cement, also known as OPC, serves as a prevalent construction material; nevertheless, its manufacturing process involves notable energy usage and results in considerable release of carbon dioxide (CO_2) into the air(H.M. and Unnikrishnan 2022; Tanu and Unnikrishnan 2023). According to reports(Gopalakrishna and Dinakar 2023) Approximately 5–7% of CO_2 emissions indicate the anthropogenic CO_2 emission of cement production, therefore, there is a critical need to explore substitute materials for OPC to mitigate the adverse impact of these emissions on the environment. Conversely, the most significant contemporary threat to humanity is global warming and environmental pollution. It is possible to transform industrial waste materials into practical construction materials(Naveen Kumar and Ramujee 2017). When each ton of cement is produced, a corresponding ton of CO_2 is released into the atmosphere, thus intensifying the issue of environmental contamination. Geopolymers are a novel class of non-metallic inorganic cementitious materials(Zhang 2024), that have attracted considerable attention as an alternative to OPC for preparing Geopolymer concrete (GPC). Geopolymer concrete utilizes a binder other than Portland cement, a major carbon emission source. Instead, it depends on a geopolymer

✉ Sudha C
sudhac@srmist.edu.in

[1] Department of Civil Engineering, SRM Institute of Science and Technology, Kattankulathur, Tamil Nadu, India

Published online: 20 August 2024

binder that triggers a chemical response in industrial by-products like ground granulated blast furnace slag (GGBS) and fly ash (FA), which have been extensively studied in numerous research investigations. Geopolymer concrete is a fundamental component for generating the geopolymer binder, contributing essential binding properties through a chemical reaction initiated by its combination with an alkali activator solution. FA, a byproduct of coal combustion in power plants, comprises various aluminosilicate materials. GGBS is a residual product from the iron and steel sector, created by rapidly cooling molten iron slag with water abundant in silica and alumina, GGBS is a fitting choice for geopolymer concrete, frequently blended with FA to augment the characteristics of the geopolymer binder. From an ecological standpoint, there is a pressing demand to develop worldwide infrastructure using industrial byproducts (Bellum, Venkatesh, and Madduru 2021). Given the substantial generation of construction and related waste materials, these resources align well with the current requirements of the construction industry. GPC is renowned for its exceptional durability, withstanding severe conditions and extreme temperatures. GPC utilizing low calcium FA has demonstrated significant cost-efficiency advantages over Portland cement concrete while also contributing to the reduction of harmful greenhouse gas emissions, which damage the environment.

The annual production of these industrial unused resources is steadily increasing, and researchers have observed relatively stable geopolymeric reactions associated with these combinations (FA-GGBS)(van Deventer et al. 2007; Duxson et al. 2007). Studies have shown that GPC operates via a unique reaction mechanism, emitting only approximately one-ninth of the CO_2 compared to traditional concrete production methods (Babaee and Castel 2016). GPC stands out as the most promising alternative to conventional cement-based concrete, offering effective solutions to environmental concerns (Phair et al. 2000). The binding characteristics of GPC(Mustafa et al. 2011) are achieved through a chemical reaction between an alkaline solution and the by-products containing high levels of aluminum (Al) and silicon (Si). In a calcium-abundant system, the reaction yields calcium alumino-silicate hydrate (C-A-S-H) gel, whereas, in a silica-rich environment, sodium alumino-silicate hydrate (N-A-S-H) gel is produced. In combined structures, both C-A-S-H and N-A-S-H gels are formed. Understanding the composition of these gels is crucial for determining the characteristics of geopolymer-based concrete (Gao et al. 2015; Park et al. 2016). In contrast to conventional approaches, geopolymer concrete doesn't necessitate water for the curing process; alternatively, it can be cured using steam or ambient air (Deb, Nath, and Sarker 2014; Jindal 2019). The utilization of FA in concrete necessitates heat curing. However, to achieve enhanced strength through ambient curing, it is recommended to replace FA with GGBS. Even though GPC must be heated to acquire its strength, an appropriate mix design can increase strength in ambient environments (Nath and Sarker 2017). Although cement-based and geopolymer concrete exhibit high compressive strength, cement concrete typically displays reduced ductility and durability, forming cracks when subjected to heavier loads.

To get the required strength in concrete, different mix proportioning techniques are used, taking into account the project's needs for durability and workability as well as the types and availability of materials, site circumstances, and material types. A detailed process for utilizing FA to create geopolymer concrete has been outlined(Gopalakrishna and Dinakar 2024). Additionally, updated guidelines for preparing GPC mixes that incorporate Indian standard codes have been put forth (Gaurav et al. 2024). GPC takes a novel technique by using FA and GGBS in place of cement completely. These materials are then activated using alkaline solutions. FA's density, particle size, and chemical makeup are different from cement's. Water is essential to the hydration process of typical cement concrete, however, with geopolymer concrete, it is released during the polymerization process. Therefore, for GPC to attain the necessary strength without sacrificing critical workability, developing a novel mix design process is imperative. Most existing or suggested mix design processes for generating GPC up until this point relied on trial-and-error techniques. The approaches either set the overall aggregate content or the fine and coarse aggregate content fully based on weight, in addition to not taking the specific gravity (SG) of the raw materials into consideration. Although a great deal of research has been done in the field of geopolymers, there isn't much available literature, particularly when it comes to the mix design element. To achieve the intended strength characteristics and feasible GPC, it is imperative to build a suitable mix design that is both logical and easy to utilize. Therefore, there isn't a practical mix design method available to create GPC that uses both GGBS and fly ash as binder materials at the same time. The many factors that go into the development of GPC make the mix design more intricate. Numerous features affect the performance and properties of GPC, including the concentration of activators (Mohammed, Ahmed, and Mosavi 2021), such as the molarity of NaOH, the ratio of silicates to hydroxides, temperature and curing duration, the activator's pH, the water-to-solids ratio, the chemical composition and type of the source material, the geopolymer system's Si to Al ratio, the mixing and resting periods, and the effect of the molar ratio of Na_2O to H_2O. These factors are crucial and complicate the mix design. This work proposes a self-designed mix design method for optimizing Geopolymer Concrete (GPC) using the IS code, which helps

to reduce the complexity of mix design. The main innovation is determining the target's strength by carefully evaluating the generated GPC mix's durability, microstructural, and mechanical properties. By streamlining the mix design process and enhancing the durability and performance of the concrete, this approach marks a significant advancement in the technology of sustainable building materials. Additionally, the RSM technique is employed to determine the best outcome from the experimental work.

2 Methodology

The goal of this research is to offer a mix design methodology to generate GPC using industrial waste materials like fly ash and GGBS with alkaline activators like sodium hydroxide and sodium silicate solutions. After casting, all specimens are chosen to be cured at the ambient temperature. Using IS code 10,262 – 2019 mix design is proposed and trials have been carried out for M40 grade, with changes in w/c ratio, alkaline solution, and variations in FA and GGBS percentage. The alkaline solution is prepared for the ratios referred to in the previous literature. The ideal target strength has been identified through multiple studies. The suggested mix's mechanical characteristics, microstructural examination, and short-term durability are examined.

3 Materials and experiments

3.1 Raw materials and mix design

The two precursors (FA (class F), GGBS) that were acquired from Ennore Thermal Power Plant and JSW Limited, as well as the alkaline solution from Kuttuva Silicates Pvt. Ltd. in Madurai, served as the raw materials for the current experimental research. GGBS, a by-product of blast furnaces in the iron-making method, exhibits high reactivity even at ambient temperature. Utilizing GGBS as the precursor in GPC proves beneficial in enhancing the workability, setting time, and early strength of fresh GPC. Moreover, it contributes to the durability of GPC by mitigating issues such as alkali-silica reactions and sulfate attacks. FA is a by-product produced through coal combustion in industrial processes. It falls into two categories based on the combined presence of aluminum, silicon, and iron oxides in the ash. Class F-FA is designated when the total exceeds 70%, while Class C is assigned when the sum ranges from 50 to 70%. Normally, Class C-FA demonstrates restrained reactivity with alkaline activators owing to its diminished glass content and heightened calcium levels. The spherical shape and diminutive particle size of FA significantly contribute to augmenting concrete density and reducing permeability. Utilizing these materials in tandem as a composite binder tends to yield greater benefits compared to their usage. Table 1 lists the chemical composition of FA and GGBS and their physical properties were determined as per ASTM C618(ASTM C618 2003)and ASTM C989 (ASTM 2006) shown in Table 2a. The alkaline solution is formed by mixing sodium hydroxide (NaOH) at a 48% concentration with a density of 2.13 g/cm^3 and sodium silicate (Na_2SiO_3) with a density of 2.61 g/cm^3. The fine aggregate used is M-sand, while the coarse aggregate consists of crushed stone ranging in size from 10 mm to 12 mm and was procured from local sources. The aggregates' physical characteristics were evaluated by ASTM C33(Standard 2018), ASTM C136/C136M-14(ASTM2014)and IS 2386 (IS 2386- Part III 1963) and are shown in Table 2b and the mix proportion of range is shown in Table 3. The images of the samples are shown in Fig. 1.

The geopolymer concrete was produced using the mix design procedure outlined in IS 10,262 – 2019(IS 10262 – 2019) exposure to ambient temperatures. The series of 25 specimens with dimensions of cube as 100 mm were meticulously prepared for compressive strength evaluation to determine the optimal mix ratio and corresponding strength by varying the w/c ratio, FA -GGBS percentage, and alkaline solution. Various permutations of alkaline and water ratios were systematically altered and examined through trial testing. After numerous trials, a final iteration yielded a specimen exhibiting a compressive strength value proximal to the target. This sample was chosen as the

Table 1 Chemical composition of FA and GGBS

Particulars	Class F-FA	GGBS
Silicon dioxide (SiO_2)	56.81	36.74
Aluminium oxide (Al_2O_2)	28.9	10.78
Iron Oxide Fe_2O_3)	10.17	0.4
Magnesium Oxide (MgO)	0.81	3.21
Calcium Oxide (CaO)	1.78	43.34
Potassium Oxide(K_2O)	1.65	0.17
Sodium oxide(Na_2O)	1.67	0.18
Sulphur trioxide (SO_3)	-	0.5
Titanium dioxide (TiO_2)	1.22	0.84
Loss on ignition	1.24	0.6

Table 2 A physical properties of FA and GGBS, B physical properties of fine aggregate and coarse aggregate

Precursor	Specific gravity	Fineness m^2/kg	Bulk density kg/m^3
FA	2.1	330	1005
GGBS	2.9	425	1350
Sl.No	Physical properties	Fine aggregate	Coarse Aggregate
1.	Specific Gravity	2.67	2.7
2.	Fineness Modulus	2.7	7.8
3.	Moisture content	5%	0.15%

Table 3 Mix proportion of GPC concrete

Mix ID	Binder content		Fine aggregate (kg/m^3)	Coarse aggregate (kg/m^3)	RGL (SSS + SHS + water) (kg/m^3)
	Fly ash(kg/m^3)	GGBS (kg/m^3)			
FG4M1	412.2	45.8	764.86	902.26	274.8
FG4M2	366.4	91.6	764.86	902.26	274.8
FG4M3	320.6	137.4	764.86	902.26	274.8
FG4M4	274.8	183.2	764.86	902.26	274.8
FG4M5	229	229	764.86	902.26	274.8

[FG4M1-FG4M5: F denotes Fly ash, G denotes GGBS,4 denotes the Grade of GPC, M (1–5) denotes the mix number, SSS-Sodium silicate solution, SHS -Sodium hydroxide solution]

Fig. 1 Images of precursor, alkaline solutions, and aggregates

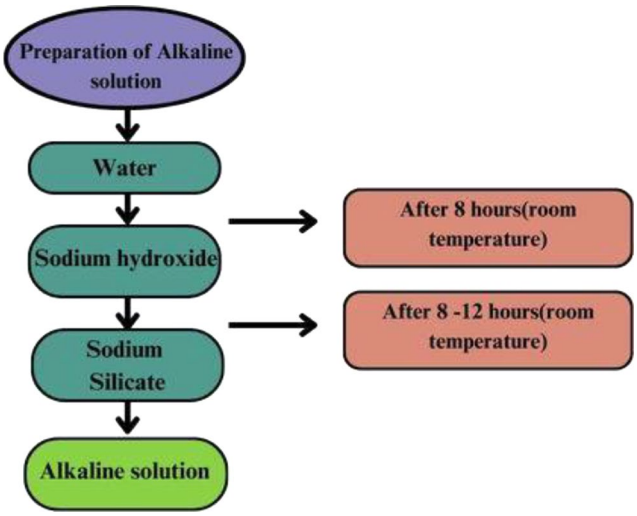

Fig. 2 Preparation of alkaline solution

standard for subsequent analysis to determine the maximum strength attainable by adjusting precursor ratios and the mix proportions of the optimal mixes were shown in Table 3. The experimental research was conducted to examine the durability and resistance to acid, chloride, and sulfate. The tests were performed using cubes and cylinders of the same size.

3.2 Preparation of alkaline activators and specimens

Alkaline activators are pivotal in the development of GPC by activating pozzolanic materials and facilitating geopolymerization reactions. The process of preparing alkaline activators entails blending alkali sources with water to create a solution. NaOH and Na_2SiO_3 are commonly used as alkali sources in this process. To prepare an alkaline solution, water, and NaOH lye should be mixed in the specified ratio and left at room temperature 26 ± 2^0c for 8 h. Subsequently, the designated ratio of Na_2SiO_3 should be added, and the mixture left undisturbed for 8–12 h before casting.

The mixing procedure begins with dry mixing of coarse aggregate, fine aggregate, FA, and GGBS using a pan mixer with a capacity of 100 kg. This dry mix was carried out for two minutes adhering to the steps depicted in Fig. 2, the alkaline solution was added to the mixer containing the solid components to initiate the wet mixing phase, which continued for five minutes. After the wet mixing procedure, the newly prepared concrete is poured into molds and exposed to one minute of vibration. Afterward, all samples within the molds were left to cure naturally at room temperature for 24 h.

3.3 Experimental program

Parameters like compressive strength, split tensile strength, and flexural strength were among the mechanical attributes of GPC that were examined. The GPC conducts mix designs to produce cubic samples with dimensions of the cube as 100 mm for evaluating compressive strength (IS 516–1959) (IS 516 1959). The compression test was conducted using a Compression Testing Machine (CTM) that had a maximum load capacity of 1000 kN and was operated with a loading speed of 2 mm per minute. Additionally, cylindrical samples measuring 100 mm in diameter and 200 mm in height are used to evaluate the splitting tensile strength (IS 5816 – 1999)(IS 5816 – 1999). Transverse loads are applied to these cylinders on the universal testing machine to determine their splitting tensile strength. Samples with dimensions of 100 mm in width, 100 mm in height, and 500 mm

in length are used to measure flexural strength. These beam specimens are subjected to a two-point load or flexural tensile test using a flexural testing machine to determine the flexural strength of the GPC mix specimen (IS 9399 – 1979) (IS 9399 1979 2004).

3.4 Characterization study

The investigation into the microstructure of GPC-cured specimens involved a comprehensive array of analytical methods, including X-ray Diffraction (XRD), Scanning Electron Microscopy (SEM), Energy Dispersive Spectroscopy (EDS), and Fourier Transform Infrared Spectroscopy (FTIR). GPC samples were carefully extracted from the inner core of cured specimens that had undergone compressive strength testing, allowing for detailed micro-level examinations. SEM images were taken with the Scanning Electron Microscope MINI-SEM SNE-3200 M, which is equipped with an energy-dispersive X-ray analysis system. This setup allows for the observation of cement-hydrated product formation and pore distribution. EDS analysis aided in identifying the elemental composition of the composite material. XRD analysis employed a PANalytical apparatus (X'pert high score plus software with ICSD) to discern crystalline and mineral phases within the composites, collecting data across a two theta (2θ) angle range from 0° to 100° at 10° intervals. FTIR analysis, performed with Bruker Alpha-T equipment, revealed information about the bonding of molecular groups in the concrete samples, covering a wavelength range from 400 to 4000 cm^{-1}.SEM images of Fly and GGBS are depicted in Figs. 3 and 4.

3.5 Response surface methodology model

Response Surface Methodology (RSM) is a structured technique used to examine the complex relationships between input factors and one or more output variables (Box and Wilson 1951). This method presents a valuable strategy for crafting accurate models, even when experimental data are scarce, especially when the output depends on numerous variables.RSM seeks to establish a significant connection between input and output variables to precisely identify the optimal operating conditions for the system under investigation(Habibi et al. 2021; Raymond H. Myers, Douglas C. Montgomery 2016). Notable experimental designs within RSM include the Box-Behnken Design (BBD), Central Composite Design (CCD), and Optimal Design (Koç and Kaymak-Ertekin 2010). Evaluating experimental data requires fitting it into statistical models like linear, quadratic, cubic, or two-factor interaction (2FI). Linear independent variables are represented by factors like A, B, and C, and two-factor and quadratic models are indicated by combinations like AB, BC, CA, A^2, B^2, and C^2. The adequacy of models is evaluated using metrics such as the coefficient of determination (R^2), adjusted R^2, and adequate precision, with a strong emphasis on the lack of fit to ensure the model's robustness. Additionally, the statistical significance of mean differences is assessed using Analysis of Variance (ANOVA) (Aydar et al. 2017).

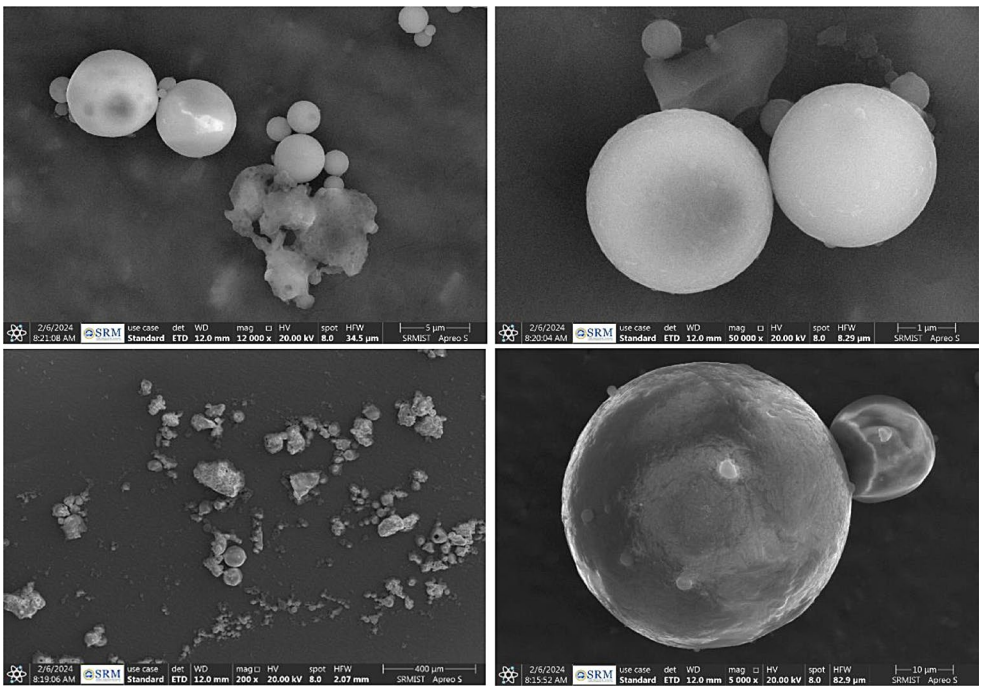

Fig. 3 SEM image of fly ash

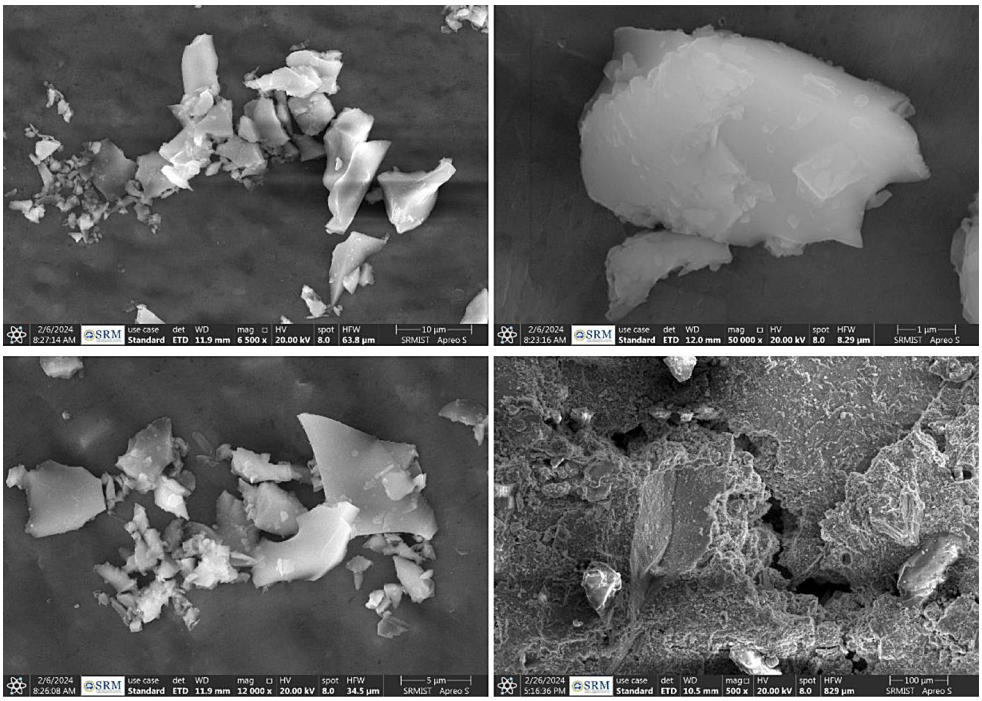

Fig. 4 SEM image of GGBS

3.6 Durability test

Tests are conducted on geopolymer concrete specimens to assess their durability through evaluations of water absorption, the volume of permeable voids, and resistance to chemical attacks such as acid, sulfate, and chloride. These evaluations provide insights into the material's ability to withstand environmental stresses and maintain structural integrity over time.

4 Result and discussion

This section provides a concise overview of the outcomes from various experimental tests detailed in the literature. The study covers mechanical aspects such as compressive strength, split tensile strength, and flexural strength. It also includes microstructural analyses conducted using XRD, SEM, and FTIR, as well as durability tests involving acid attack, sulfate attack, and chloride attack. Additionally, the study examines water absorption rates, volume of permeable voids, and utilizes RSM to predict compressive strength, comparing experimental findings with actual values.

4.1 Mechanical properties of GPC

4.1.1 Compressive strength

The results indicate that as the percentage of GGBS in Fly Ash-based GPC increases, the strength also increases,

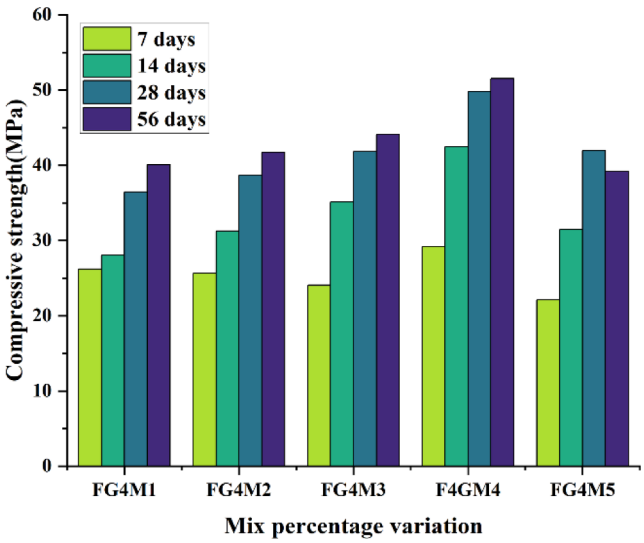

Fig. 5 Compressive strength of GPC

but the target strength is not achieved within the 0–30% replacement range. The desired strength level is attained at a 40% GGBS replacement in FA, particularly in mix FG4M4, which demonstrates optimum strength characteristics. Notably, the highest compressive strength is recorded on 28 and 56 days, with values for FG4M4 reaching 29.19, 42.45, 49.81, and 51.52 MPa, indicating the effectiveness of the optimal mix and it is illustrated in Fig. 5. In general, the compressive strength rises as the GGBS % increases. An increase in compressive strength of about 17% yields the maximum strength. However, beyond 28 days, the compressive strength experiences only a slight rise, approximately

2–5%, from 28 days to 56 days. Earlier investigations have shown that the inclusion of GGBS as a primary component in GPC enhances its strength when subjected to room temperature conditions (Amin et al. 2022; Sethi, Bansal, and Sharma 2019). Furthermore, research suggests(Oyebisi et al. 2020)that higher concentrations of sodium hydroxide result in heightened compressive strength, as increased molarities of alkaline solutions, contain a greater number of dissolved aluminosilicates. As a result, the polymerization process proceeds more quickly, which eventually improves the mechanical strength characteristics of geopolymer concrete.

4.1.2 Split tensile strength

The splitting tensile strength, sometimes called indirect tensile strength, is determined by applying static lateral loading to cylindrical specimens using the Universal Testing Machine (UTM). The split tensile strength is assessed after 7, 28, and 56 days of curing under ambient conditions, depicted in Fig. 6. The split tensile strength of geopolymer concrete prepared using M40 displays a similar pattern to the compressive strength at various replacement levels. Test results indicate a tendency for split tensile strength to decrease with increasing GGBS replacement. Notably, the FG4M4 mixture demonstrates higher strength, achieving values of 5.16 MPa and 5.44 MPa at 28 and 56 days, respectively, under ambient curing conditions. Tensile strength rises as GGBS replacement reaches 40% but declines with higher replacement percentages. There is a correlated increase in tensile strength with the augmentation of GGBS content, typically by around 2–3%.

4.1.3 Flexural strength

Concrete's flexural strength generally demonstrates a higher value than its splitting tensile strength (Nath and Sarker 2017). The results concerning the flexural strength (modulus of rupture) of the GPC are shown in Fig. 7. The flexural strength demonstrates a similar pattern to the compressive strength and split tensile strength at all substitution levels. The experimental data suggests that the flexural strength tends to decline as the proportion of GGBS increases, reaching its highest point at a 40% replacement rate, aligning with the observed trend in other mechanical properties. In the case of GPC, the FG4M4 mix demonstrated flexural strengths of 5.16 MPa and 7.14 MPa at 28 and 56 days, respectively. With prolonged curing, there is an approximate 2% enhancement in flexural strength. Comparatively, the FG4M4 mixture displayed a strength increase of 2–4% when contrasted with mixes FG4M1-FG4M3 and FG4M5.

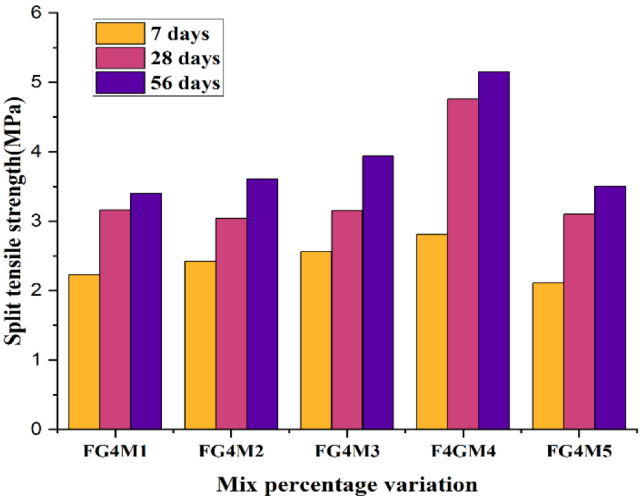

Fig. 6 Split tensile strength of GPC

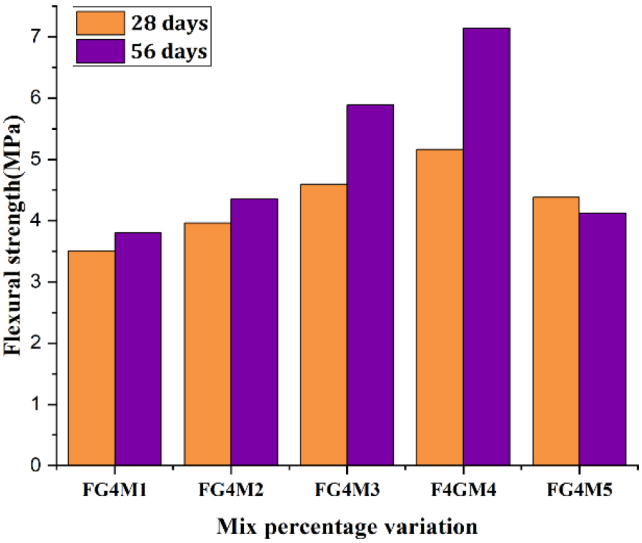

Fig. 7 Flexural strength of GPC

4.2 Microstructure analysis

4.2.1 X-Ray diffraction analysis (XRD)

The preeminent crystalline peak observed in the figure corresponds to quartz (SiO_2), exhibiting a notable intensity at an angle of $2\theta = 26^{o}$. This observation is substantiated by X-ray fluorescence (XRF) analysis, which quantifies the SiO_2 content at 56.81% and aligns with the literature values, which commonly report similar peaks for quarts in GGBS and FA based materials(Jangid, Choudhary, and Balotiya 2023). Furthermore, mullite ($Al_6O_{13}Si_2$) emerges as another salient peak, detected across multiple 2θ ranges, specifically at 16° and 67° degrees. In Fig. 8, the mineral composition of GGBS is delineated, indicating the presence of Quartz (SiO_2) and Calcium carbonate ($CaCO_3$) as the primary

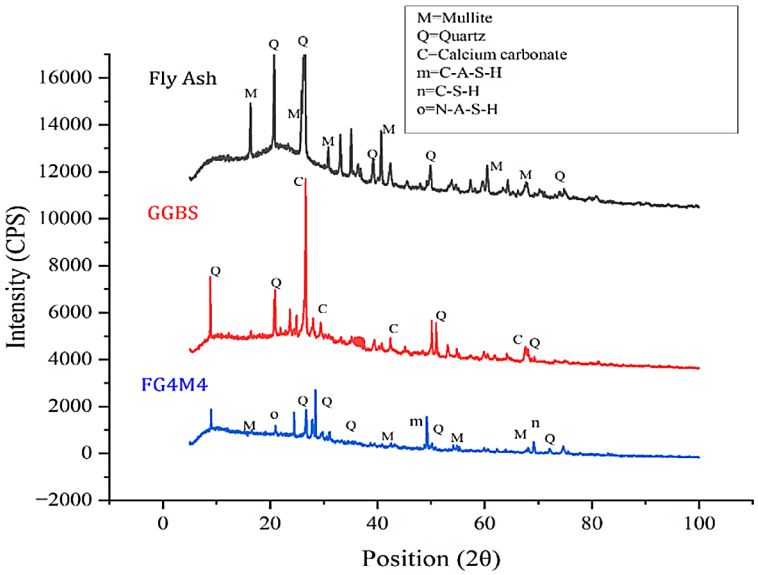

Fig. 8 XRD pattern of fly ash, GGBS, and FG4M4 at 28 days curing period

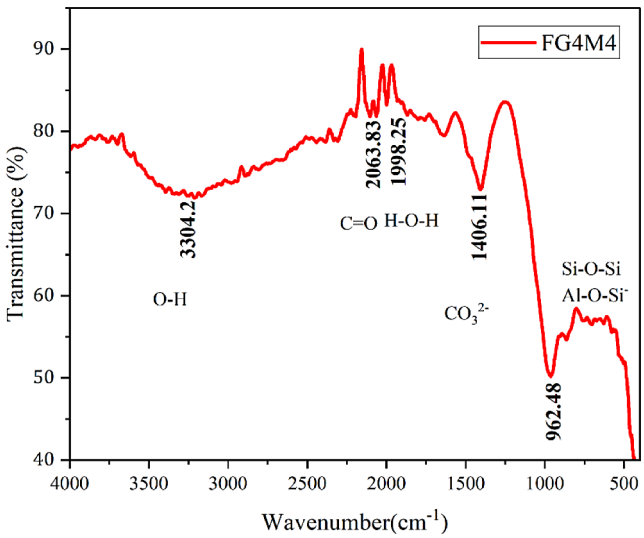

Fig. 9 FTIR analysis of FG4M4 of GPC at the 28th day curing period

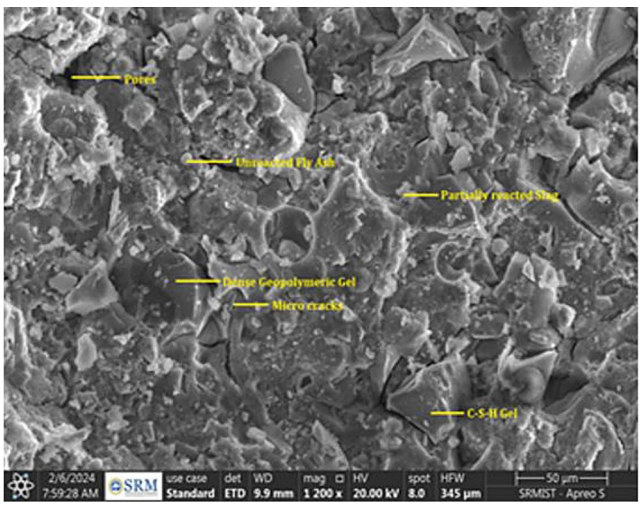

Fig. 10 SEM characterization of the geopolymer concrete

constituents. Notably, calcium carbonate registers a peak at 2θ = 27° where reports(Chary and Munilakshmi 2024) finds that $CaCO_3$ frequently report around this angle, while quartz displays peaks within the range of 25–60°. The X-ray diffraction (XRD) patterns of the FA-based geopolymer concrete (GPC), cured at room temperature as depicted in Fig. 8, display multiple clear peaks, suggesting the presence of crystalline phases within the material. Aluminosilicate substances exhibiting an amorphous configuration constitute the principal polymerization byproducts synthesized within geopolymer matrices, specifically denoted by way of N-A-S-H and C-A-S-H. Therefore, the predominant constituents of FG4M4 X-ray diffraction (XRD) pattern consist of a broad amorphous peak attributed to aluminosilicate at 2θ = 28°, alongside a minor presence of low-crystalline calcium-silicate-hydrate (C-S-H) gel.

4.2.2 Fourier transform infrared spectroscopy (FTIR)

FT-IR spectroscopy, an analytical technique, aims to identify primary reaction sites involving Si–O and Al–O within cementless paste. The chemical bonds within the FG4M4 mixture were analyzed using FTIR within the mid-IR spectrum (4000 cm-1 to 400 cm^{-1}) is shown in Fig 9. Observations suggest (Barbosa, MacKenzie, and Thaumaturgo 2000)that reactions primarily occur below 1200 cm^{-1}. Milkey(Milkey 1960) noted a correlation between polymerization-induced peak frequencies and increased Al component quantities relative to the Si: Al ratio. Stretching vibrations associated with O–H bending was observed at 3304.2 cm^{-1}, same peak associated with the water and hydroxyl group was reported by Jangid et al., (Jangid et al. 2023). The peak observed at 2063.83 cm^{-1} in the stretching vibration spectrum suggests the formation of C = O

bonds, indicating the potential presence of CO_2. The peaks at 1998.25 cm-1 indicate the presence of hydroxyl groups (HO-H) aligning with literature that identifies these features around 2000 cm^{-1}(Tushar et al. 2022). Carbonate (CO3) stretching vibrations were observed at 1406.11 cm-1. The broad peak at 962.48 cm-1 corresponds to the asymmetric and symmetric stretching vibrations of Si-O-Si and Al-O-Si bonds, typically associated with the formation of C-S-H gel during the dissolution of SiO4 tetrahedra(Fernandez-Jimenez and Puertas 2003; Yunsheng et al. 2007).

4.2.3 Scanning electron microscopy (SEM)

SEM and EDS analyses were conducted on the optimum mix to discern the reactants influenced by the alkaline activator. Furthermore, they aimed to confirm the internal microstructure of the sample. The SEM images of geopolymer Concrete for the optimum mix (FG4M4) at the curing age of 28 days are shown in Fig. 10. Key microstructural characteristics include gel formation, unreacted FA particles, partially reacted FA, and GGBS, as well as microcracks and pores. The aluminosilicate gel formed through polymerization in geopolymers can be observed. Figure 11 illustrates the EDS analysis of specimens after 28 days of aging, with the corresponding weight ratios provided in Table 4. The accompanying table displays the quantitative elemental analysis from the EDS spectrum. It indicates that silicon (17.53% by weight, 12.42% by atom) and oxygen (49.26% by weight, 61.25% by atom) constitute the majority of the sample's composition, indicating that the material may be silicate. Notable quantities of calcium (10.91% by weight), aluminum (6.98% by weight), and salt (6.04% by weight) are also present. Minor elements include iron, sulfur, magnesium, potassium, titanium, and carbon; carbon makes up around 4.89% of the weight. The data illustrates the heterogeneous structure of the sample, which is mainly composed of silicon and oxygen, with other elements contributing to the remaining material. In FA-based geopolymers, alkali activation initiates the formation of N-A-S-H gel. On the other hand, in geopolymers composed of both FA and ground granulated blast furnace slag (GGBS), the high pH environment promotes the replacement of sodium ions with calcium ions from the GGBS. This process results in the precipitation of C-A-S-H or C-S-H phases until the calcium is exhausted. As a result, the geopolymer displays a mixture of N-A-S-H, C-S-H, and C-A-S-H phases (Puligilla and Mondal 2013). Research has shown that unused particles don't just fill space; they make the material stronger over time by helping it bond better through complicated surface reactions (Kumar et al. 2007; Xu and Van Deventer 2000).

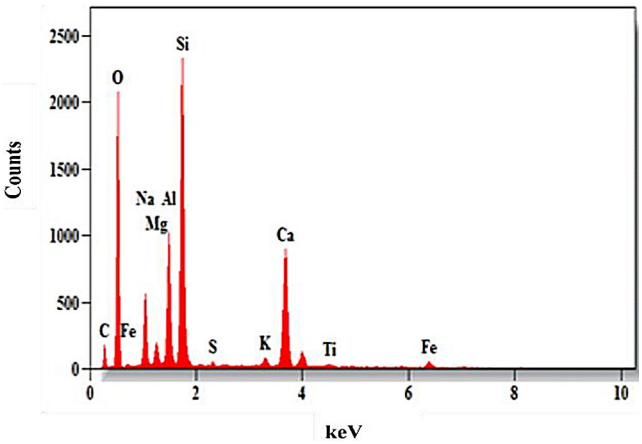

Fig. 11 Microstructural characterization using SEM

Table 4 Chemical composition analysis of optimum mix from EDS

Element & formula	Net counts	Weight%	Atom %	Atom % error
C	899	4.89	8.11	±0.35
O	11,461	49.26	61.25	±0.61
Na	3866	6.04	5.23	±0.12
Mg	1315	1.52	1.25	±0.06
Al	7809	6.98	5.14	±0.10
Si	20,319	17.53	12.42	±0.11
S	270	0.22	0.14	±0.02
K	613	0.58	0.30	±0.02
Ca	10,545	10.91	5.41	±0.06
Ti	379	0.57	0.24	±0.04
Fe	623	1.50	0.54	±0.08
Total	58,102	100.00	100.00	±1.57

SEM images reveal a decrease in crystallinity during the geopolymerization process of GGBS and FA-based concrete. The transition from well-defined crystalline structures to a more uniform, amorphous gel matrix corresponds to the reduction in crystallinity observed in XRD analysis. This change is in line with the development of non-crystalline phases that disrupt the structure of the original materials, such as N-A-S-H and C-A-S-H. The dissolution of crystalline phases, such as quartz and mullite, and the resulting polycondensation reactions result in the formation of a mostly amorphous matrix. This observation emphasizes the efficient process of transforming precursor materials into a geopolymeric network, resulting in enhanced mechanical properties of GPC concrete.

4.3 Relation between compressive strength, flexural strength, and split tensile strength

This section examines the relationship between compressive strength, flexural strength, and split tensile strength in geopolymer concrete, emphasizing their strength properties

after 28 days of curing. Predicting flexural and split tensile strengths from the achieved compressive strength can be beneficial (Kaveh and Khavaninzadeh 2023). Figure 12 visually presents the relationship between compressive strength, flexural strength, and split tensile strength. This figure includes equations that estimate the flexural and split tensile strengths of GPC based on its compressive strength. Using the equations, one can calculate the flexural and split tensile strengths of GPC from its compressive strength. These proposed mathematical model equations are labeled as Eqs. 2 and 3.

$$Y = 2.3392 + 0.1493x \tag{2}$$

$$Y = 0.6701 + 0.1195x \tag{3}$$

In this context, Y symbolizes both flexural strength & split tensile strength, while x denotes compressive strength. As a result, the developed model equation enables the prediction of the compressive strength of geopolymer concrete in this study.

4.4 RSM analysis

In the analysis of the research data, RSM is utilized to evaluate and develop predictive models for the compressive strength of GPC) on the 28th day. Table 5 presents an overview of the design considerations for the RSM approach. It encompasses 12 experiments, incorporating trial and failure responses, with a quadratic model applied for the design.

$$\begin{aligned} Compressive\ strength = & -221.44 - 33.95A \\ & + 16.09B + 232.54C \\ & + 36.85310A - 137.45A.C \\ & - 20.19B.C \end{aligned}$$

The model achieved a high level of statistical significance (F-value = 41.74, $p < 0.0005$), evidencing that the factor combinations considerably affect compressive strength. Individually, the factors B-SH and C-SS, along with the interaction effects of AB, AC, and BC, were statistically significant ($p < 0.01$), illustrating their strong influences on compressive strength. In contrast, the water ratio (A) did not exhibit a significant impact ($p > 0.05$) on compressive strength. The lack of fit test resulted in an insignificant outcome when compared to pure error (F-value = 5.76, $p = 0.1516$), suggesting the model's adequacy in capturing

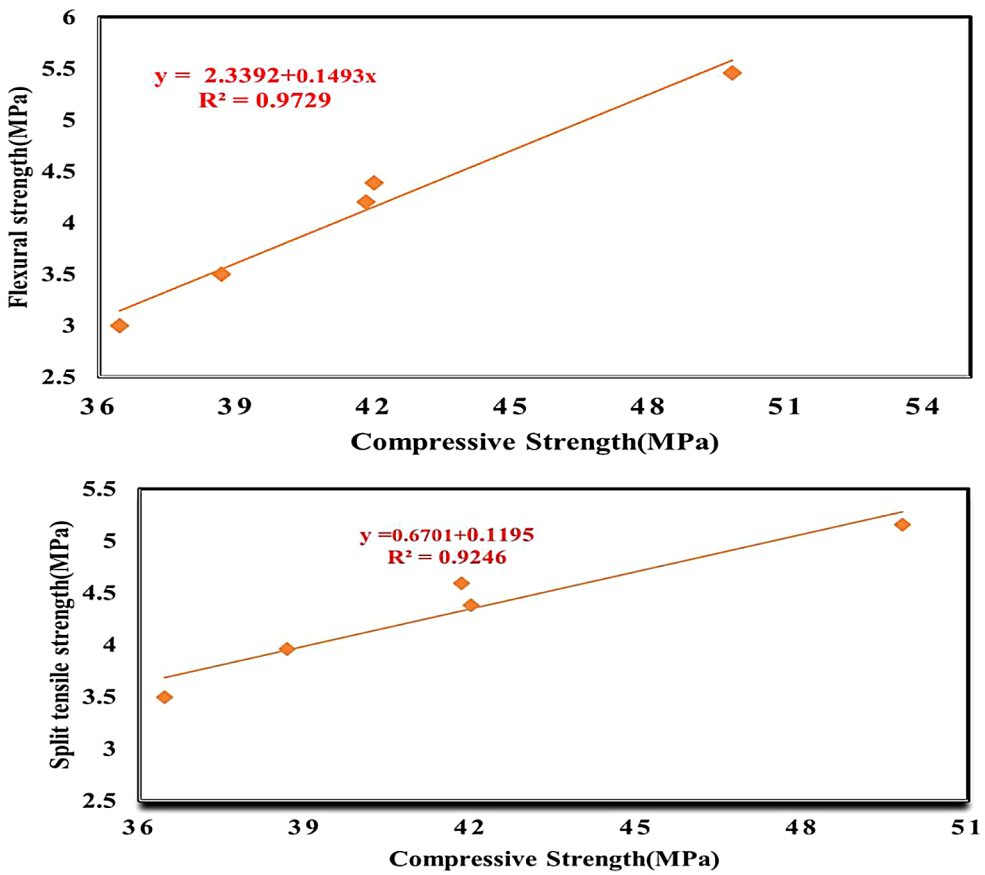

Fig. 12 Linear regression results

Table 5 Formulation of response surface methodology (RSM)

Software version.	13.0.5.0		
Type of Study	Response Surface	**Subtype**	Randomized
Type of Design	Blank Spreadsheet	**No.of.Runs**	12
Design model	Quadratic	**Blocks**	No blocks

The R^2 value of 0.9804 indicates that about 98.04% of the variance in the response variable is explained by the independent variables in the model, demonstrating a strong fit between the model and the observed data. This high R^2 value suggests that the model effectively captures a significant portion of the response's variability. The adjusted R^2, which is 0.9569, accounts for the number of predictors and provides a more conservative estimate of the model's explanatory power. Although slightly lower than the R^2 value, the adjusted R^2 still indicates a robust explanatory power of the model. The predicted R^2, at 0.1145, reflects the model's performance in predicting unseen data, suggesting potential limitations in extrapolating beyond the observed range. The adequacy precision value of 20.8173 serves as a signal-to-noise ratio, indicating the reliability of the model in capturing response variability while minimizing random fluctuations. Overall, the RSM analysis demonstrates a strong relationship between variables and the response, supported by high R^2 and adjusted R^2 values. However, caution is advised in extrapolating predictions beyond the observed data due to the lower predicted R^2 value. The high adequacy precision value underscores the model's reliability within the observed data range. Table 6 shows the fit statistic of this model. The predictive formula for compressive strength is as follows:

Table 6 Regression analysis in response surface methodology (RSM)

Std.dev.	1.01	R^2	0.9804
Mean	40.24	Adjusted R^2	0.9569
CV%	2.50	Predicted R^2	0.1145
		Adeq Precision	20.8173

Table 7 Results from ANNOVA

Source	SS	df	MS	F-value	*p*-value
Model	254.17	6	42.36	41.74	0.0004
A-water ratio	0.7533	1	0.7533	0.7423	0.4283
B-SH	18.25	1	18.25	17.99	0.0082
C-SS	113.71	1	113.71	112.05	0.0001
AB	74.34	1	74.34	73.25	0.0004
AC	74.83	1	74.83	73.74	0.0004
BC	65.57	1	65.57	64.61	0.0005
Residual	5.07	5	1.01		
Lack of Fit	4.55	3	1.52	5.76	0.1516
Pure error	0.5267	2	0.2633		
Cor Total	259.24	11			

the data. Table 7 presents the distinctive findings from a response surface methodology (RSM) analysis of variance conducted for the 28-day compressive strength and the model is significant.

Figure 13 presents a three-dimensional plot generated using Response Surface Methodology (RSM), a statistical technique used to examine the relationship between various design parameters of the mixes and the proportions of the alkaline ratio.The graph visually demonstrates that as both the water ratio in the design mix and the alkaline ratio increase, there is a corresponding improvement in compressive strength. Furthermore, Table 8 showcases the experimental and estimated values of compressive strength. Figure 13 also portrays contour plots along with the actual and predicted values obtained through RSM analysis. The figures demonstrate a close match between the observed and predicted response values.

Table 8 Actual and predicted values from RSM

Run order	Actual value	Predicted value of RSM
1	44.10	44.65
2	36.70	36.58
3	36.10	36.09
4	40.30	38.51
5	39.10	38.97
6	44.80	44.65
7	36.30	36.78
8	45.10	44.65
9	40.80	41.72
10	36.40	36.64
11	49.81	49.85
12	33.40	33.83

4.5 Durability test

Durability is the capacity of concrete to endure adverse conditions, such as weathering, abrasion, and chemical exposure while maintaining its intended technical properties for an extended period without experiencing significant degradation. FG4M4 specimens were initially cured for 28 days under ambient conditions to assess their durability properties, including resistance to acid attack, sulfate attack, chloride attack, water absorption, and the volume of permeable pore voids.

4.5.1 Acid attack, sulfate attack, chloride attack

The durability of the FA-GGBS based geopolymer concrete mix, FG4M4, was evaluated through testing. This was followed by immersion in solutions containing 5% acid, sulfate, and chloride concentrations. Following ASTM C-267(International 2020) norms, the acid resistance investigation was carried out. The ability of concrete to resist deterioration in an acidic environment is known as acid resistance. In contrast, the ability to protect against sulfate ion penetration, which can cause concrete to deteriorate and lose strength, is known as sulfate resistance. Comparably, "chloride resistance" in concrete describes the material's ability to resist the infiltration and detrimental effects of chloride ions, frequently present in seawater, deicing salts, and marine environments. The concrete samples were initially weighed after a 28-day curing period, followed by submersion in solutions containing acid, sulfate, and

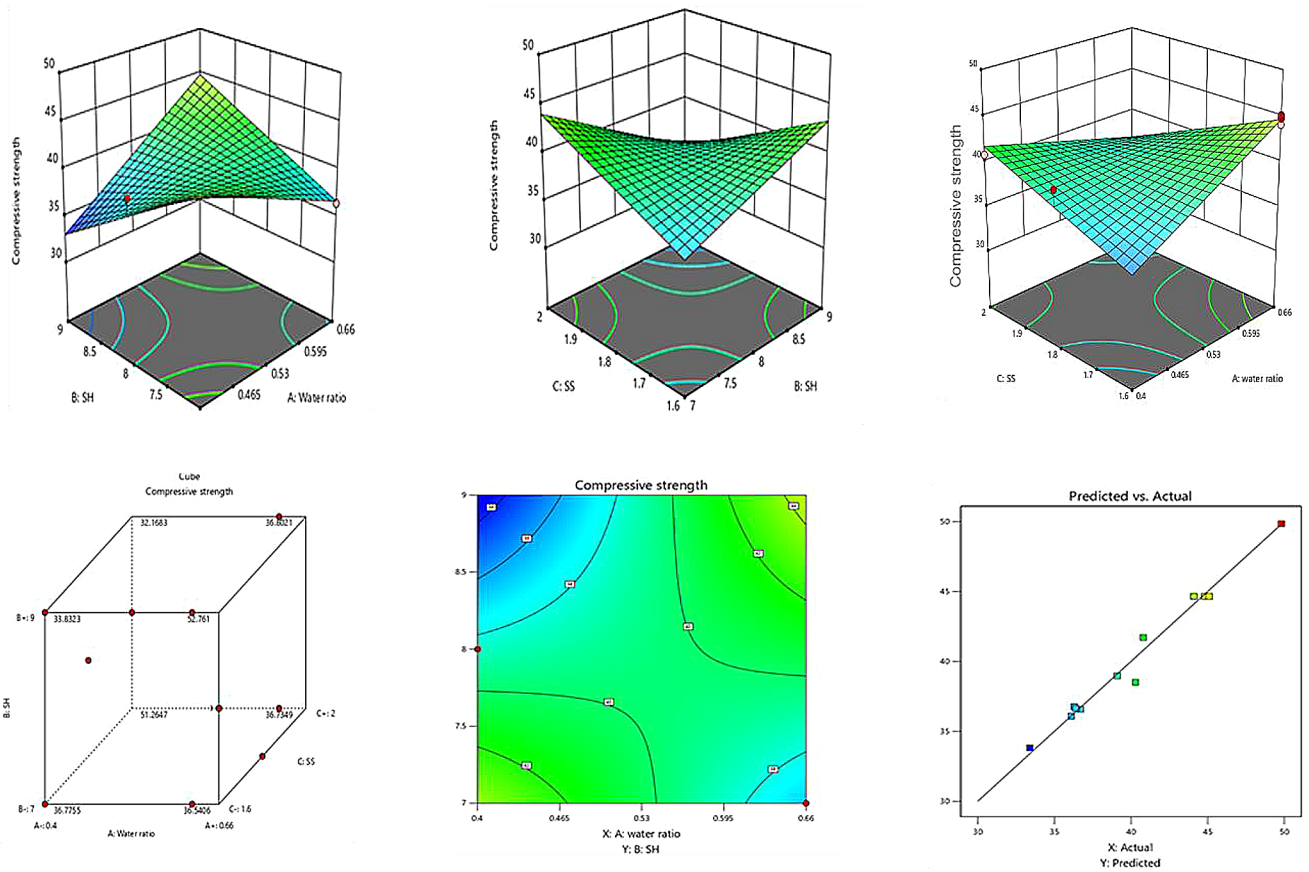

Fig. 13 3D Graph plot and cube of compressive strength using RSM

Table 9 Weight and compressive strength change in resistance to acid, sulfate, and chloride

Mix	Immersion days	Acid attack		Sulphate attack		Chloride attack	
		Loss or gain % of weight	Loss or gain % of compressive strength	Loss or gain % of weight	Loss or gain % of compressive strength	Loss or gain % of weight	Loss or gain % of compressive strength
FG4M4	30	-0.08	-4.91	0.28	-3.27	0.21	1.21
	60	-0.28	-9.93	-0.59	5.59	0.16	4.03
	90	-0.166	-11.68	0.008	8.39	0.33	6.28

chloride. After immersion periods of 30, 60, and 90 days, the resulting residual compressive strength and mass loss were evaluated and shown in Table 9.

According to the outcome, the resistant acid's weight and compressive strength have somewhat decreased. After 90 days, there is a maximum weight loss of -0.28% and a maximum reduction in compressive strength of -11.68%. This suggests a moderate sensitivity to acidic conditions, which can result in a progressive loss of structural integrity. In general, resistance to sulfate shows a slight rise in weight. Both increases and decreases in compressive strength have been observed, indicating a mixed reaction. After 90 days, the material's compressive strength increases by 8.39%, indicating that it becomes stronger over time when subjected to sulfate conditions and chloride resistance. Over time, there is a slight increase in both compressive strength and weight. After 90 days, the compressive strength increases at the greatest rate of 6.28%. This suggests that the material performs well when exposed to chlorides, improving its structural characteristics. These findings imply that geopolymer concrete is reasonably durable in a variety of environmental settings. Although the material exhibits resilience in sulfate and chloride settings, where there are only slight fluctuations in weight and an overall gain in compressive strength, acidic circumstances result in a drop in both weight and compressive strength. Researchers Lavanya et al.,(Lavanya and Jegan 2015)Mehta et al.,(Mehta and Siddique 2017)

Bakhrev T(Bakharev 2005), and Sunagar P et al.(Sunagar et al. 2021) discovered similar results.

4.5.2 Water absorption and volume of permeable voids test (VPV)

The results of the water absorption and permeability void volume (VPV) tests for the ideal mix FG4M4, assessed according to ASTM C642-21, are presented in the table below. These results include the excess dry weight, surface-dry weight after immersion, and VPV measurements following submersion in boiling water. Table 10 summarizes the findings along with the corresponding calculations.

A modest ability for water intake is indicated by the water absorption result of 4.86% for mix FG4M4, which is an important criterion in assessing the durability of concrete. According to earlier research(Thokchom, Ghosh, and Ghosh 2009), excessive water absorption in concrete can speed up deterioration processes like chemical attacks and freeze-thaw cycles, which weaken concrete structures and eventually increase maintenance costs. Furthermore, the porous nature of the material is shown by the 9.73% stated volume of permeable voids in FG4M4. While some porosity is good for increasing permeability and workability, too many voids can have a detrimental effect on mechanical qualities including compressive and flexural strengths(Wang et al. 2020)(Chen, Wu, and Zhou 2013).Concrete performance mostly depends on lower density and durability, both of which are associated with bigger void volumes(Singh et al. 2024). The authors examined how GGBS influences the properties of fly ash-based geopolymer concrete. (Guo et al. 2010; Nath and Sarker 2014). Like the FG4M4 mix results, they observed water absorption values between 4% and 6% and VPV (voids content) values between 8% and 11%. Thus, even with a sizable number of permeable areas, the results imply that FG4M4 exhibits a well-balanced mix design regarding porosity and density. To lower the void content while keeping the right amounts of water absorption and prolonging the life of concrete structures, more modifications can be required.

5 Conclusion

The research encompassed an extensive exploration of material characterization employing SEM, EDS, XRD, and FT-IR examinations. Furthermore, it encompassed the formulation of an innovative mix design and evaluation of the mechanical characteristics of GPC derived from FA and GGBS under ambient curing circumstances, the short-term durability properties were also tested. Furthermore, the study explored the relationship between mechanical properties and the compressive strength of GPC predicted using RSM. Based on the findings the following conclusions were drawn:

- The study explored the effects of partially replacing FA with GGBS in different experimental mixes on the flexural, split tensile, and compressive strengths of GPC. Remarkably, the FG4M4 mix, consisting of 60% GGBS and 40% FA, exhibited superior mechanical characteristics. Compressive strength improved by 17% with minor improvements of 2–5% from 28 to 56 days in the FG4M4 mix. Tensile strength increased by 2–3% with greater GGBS content, and flexural strength increased by 2% over time with FG4M4 showing a 2–4% increase.
- XRD analysis was utilized to examine the crystalline structure, revealing peaks of quartz (SiO_2) and mullite ($Al_6O_{13}Si_2$), indicative of the formation of alumina-silicate substances with an amorphous structure during geopolymerization.
- The Fourier Transform Infrared (FTIR) analysis corroborated the enhanced mechanical performance of GPC upon the partial substitution of fly ash with GGBS.
- The SEM-EDS examination confirmed the existence of Si, Al, Ca, and Na-essential elements in the formation of geopolymeric gels. Additionally, it verified the presence of pores, cracks, unreacted slag, and fly ash within the polymeric gel matrix.
- RSM investigations yielded a high R^2 value of 0.98 for compressive strength prediction, indicating the reliability of the models in forecasting compressive strength.
- This research assesses the durability of geopolymer concrete in diverse settings, emphasizing its advantages and disadvantages. Weight (-0.28%) and compressive strength (-11.68%) show a significant decline under acidic circumstances over ninety days, suggesting a moderate degree of sensitivity and possible problems

Table 10 Results of VPV and water absorption analysis

Mix id	Weight of oven-dried specimen (kg)	Weight of the specimen after immersion in water(kg)	Weight of the specimen after 5 h of boiling(kg)	Saturated weight of the specimen(kg)	Water absorption	The volume of permeable voids
FG4M4	1.706	1.789	1.782	1.001	4.86	9.73

with structural integrity. However, under sulfate circumstances, the material shows irregular compressive strength responses and a slight weight increase, with an average increase of 8.39% observed. The maximum improvement in compressive strength over the same period seen in settings rich in chlorides is 6.28%.

- The study emphasizes how crucial permeability and porosity are to the functionality of concrete. With a moderate water absorption rate of 4.86%, Mix FG4M4 satisfies durability requirements by reducing the possibility of chemical attacks and freeze-thaw cycles. FG4M4 exhibits a balanced porosity and density design with 9.73% permeable voids, comparable to findings with GGBS in geopolymer concrete. Optimizing mix designs to minimize void content while preserving appropriate amounts of water absorption is essential to improving the structural resilience and lifespan of concrete.

Combining FA and GGBS with GPC presents an effective approach to constructing environmentally friendly structures. Prioritizing mix design optimization in future research endeavors is essential to enhancing the mechanical properties of GPC. Moreover, exploring various combinations of precursor materials and activators offers opportunities for tailoring concrete mixes to specific technical requirements and environmental conditions. Implementing regulatory requirements and standards specific to fly ash and GGBS-based GPC will further facilitate its widespread adoption and integration into construction projects.

Author contributions First author : Conducted experiments, collected data. Contributed to writing the methodology section.Corresponding author : Conceptualization, methodology, and supervision of the research. Responsible for overall project direction and coordination.

Data availability No datasets were generated or analysed during the current study.

Declarations

Competing interests The authors declare no competing interests.

References

Amin M, Elsakhawy Y Khaled Abu el-hassan, and Bassam Abdelsalam Abdelsalam. 2022. Behavior evaluation of sustainable high strength geopolymer concrete based on fly Ash, Metakaolin, and Slag. Case Stud Constr Mater 16:e00976. https://doi.org/10.1016/j.cscm.2022.e00976

ASTM C (2006) Standard specification for Ground Granulated Blast furnace slag for use in concrete and mortars. 402:8–10

ASTM C618, USA (2003) Standard Specification for Coal Fly Ash and Raw or Calcined Natural Pozzolan for Use in Concrete // ASTM International: West Conshohocken, PA,. 2019. 14(200):4–5. https://doi.org/10.1520/C0618-17A.10.1520/C0618-19.2

ASTM A, C136/C136M–14 (2014) Standard Test Method for Sieve Analysis of Fine and Coarse aggregates. ASTM International, West Conshohocken, PA.

Aydar AY, Bağdatlıoğlu N, Köseoğlu O (2017) Effect of Ultrasound on Olive Oil Extraction and Optimization of Ultrasound-Assisted Extraction of Extra Virgin Olive Oil by Response Surface Methodology (RSM). Grasas Aceites 68(2):189. https://doi.org/10.3989/gya.1057162

Babaee M, Castel A (2016) Chloride-Induced corrosion of reinforcement in low-calcium fly Ash-based geopolymer concrete. Cem Concr Res 88:96–107. https://doi.org/10.1016/j.cemconres.2016.05.012

Bakharev T (2005) Resistance of Geopolymer materials to Acid Attack. Cem Concr Res 35:1233–1246

Barbosa VFF, Kenneth JD, MacKenzie, and Clelio Thaumaturgo (2000) Synthesis and characterisation of materials based on inorganic polymers of Alumina and silica: Sodium Polysialate polymers. Int J Inorg Mater 2(4):309–317. https://doi.org/10.1016/S1466-6049(00)00041-6

Bellum R, Reddy C, Venkatesh, Madduru SRC (2021) Influence of red mud on performance enhancement of fly Ash-based geopolymer concrete. Innovative Infrastructure Solutions 6(4):215. https://doi.org/10.1007/s41062-021-00578-x

Box GEP, Wilson KB (1951) On the experimental attainment of Optimum conditions. J Royal Stat Soc Ser B: Stat Methodol 13(1):1–38. https://doi.org/10.1111/j.2517-6161.1951.tb00067.x

Chary KS, and Nijagala Munilakshmi (2024) Experimental studies on improving the potential properties using Eggshell Powder based Geopolymer concrete with sustainable materials. Innovative Infrastructure Solutions 9(6). https://doi.org/10.1007/s41062-024-01506-5

Chen X, Wu S, and Jikai Zhou (2013) Influence of Porosity on Compressive and Tensile Strength of Cement Mortar. Constr Build Mater 40:869–874. https://doi.org/10.1016/j.conbuildmat.2012.11.072

Deb P, Sarathi P, Nath, and Prabir Kumar Sarker (2014) The effects of Ground Granulated blast-furnace slag blending with fly Ash and Activator Content on the workability and Strength properties of Geopolymer concrete cured at ambient temperature. Mater Des (1980–2015) 62:32–39. https://doi.org/10.1016/j.matdes.2014.05.001

Duxson P, Provis JL, Lukey GC, Jannie SJ, van Deventer (2007) The role of Inorganic Polymer Technology in the development of 'Green concrete'. Cem Concr Res 37(12):1590–1597. https://doi.org/10.1016/j.cemconres.2007.08.018

Fernandez-Jimenez A, Puertas F (2003) Effect of Activator Mix on the hydration and strength behaviour of Alkali-activated slag cements. Adv Cem Res 15(3):129–136. https://doi.org/10.1680/adcr.15.3.129.36623

Gao X, Yu QL, Brouwers HJH (2015) Reaction kinetics, gel character and strength of ambient temperature cured Alkali activated slag–fly Ash blends. Constr Build Mater 80:105–115. https://doi.org/10.1016/j.conbuildmat.2015.01.065

Gaurav J, Modhera C, Patel D (2024) Proposed Mixture Design Method for High-Strength Geopolymer concrete. ACI Mater J 121(1):67–78. https://doi.org/10.14359/51739201

Gopalakrishna B, and Pasla Dinakar (2023) Mix Design Development of fly Ash-GGBS Based Recycled Aggregate Geopolymer concrete. J Building Eng 63:105551. https://doi.org/10.1016/j.jobe.2022.105551

Gopalakrishna B, and Pasla Dinakar (2024) An innovative Approach to fly Ash-based Geopolymer concrete Mix Design: utilizing 100% recycled aggregates. Structures 66. https://doi.org/10.1016/j.istruc.2024.106819

Guo X, Shi H, Dick WA (2010) Compressive strength and microstructural characteristics of Class C fly Ash Geopolymer. Cem

Concr Compos 32(2):142–147. https://doi.org/10.1016/j.cemconcomp.2009.11.003

Habibi A, Ramezanianpour AM, Mahdikhani M, Bamshad O (2021) RSM-Based evaluation of Mechanical and Durability properties of recycled aggregate concrete containing GGBFS and silica fume. Constr Build Mater 270:121431. https://doi.org/10.1016/j.conbuildmat.2020.121431

International ASTM (2020) ASTM C267 - standard test methods for Chemical Resistance of mortars. Grouts, and Monolithic Surfacings and Polymer Concretes.

IS 10262–2019 (2019) Indian Standard, Concrete Mix Proportioning – Guidelines (Second Revision). Pp. 1–42 in *Bis*

IS, 2386- Part III (1963) Method of Test for Aggregate for Concrete. Part III- Specific Gravity, Density, Voids, Absorption and Bulking. *Bureau of Indian Standards, New Delhi* (Reaffirmed 2002)

IS 516 (1959) Method of tests for strength of concrete. Bureau Indian Stand 1–30

IS 5816–1999 (1999) Indian Standard Splitting Tensile strength of concrete- method of test. Bureau Indian Stand 1–14

IS 9399 1979 (2004) Specification for Apparatus for Flexural Testing of Concreting. Bureau Indian Stand 1–13

Jangid S, Kr R, Choudhary, and Manoj Balotiya (2023) Performance analysis of GGBS and fly Ash-based geopolymer concrete. Smart Innov Syst Technol 334:597–604. https://doi.org/10.1007/978-981-19-8497-6_54

Jindal BB (2019) Investigations on the properties of Geopolymer Mortar and concrete with Mineral admixtures: a review. Constr Build Mater 227:116644. https://doi.org/10.1016/j.conbuildmat.2019.08.025

Kaveh A, and Neda Khavaninzadeh (2023) Efficient training of two ANNs using four Meta-Heuristic algorithms for Predicting the FRP Strength. Structures 52:256–272. https://doi.org/10.1016/j.istruc.2023.03.178

Koç B (2010) and Figen Kaymak-Ertekin. Response Surface Methodology and Food Processing Applications.

Kumar R, Kumar S, Mehrotra SP (2007) Towards sustainable solutions for fly Ash through Mechanical activation. Resour Conserv Recycl 52(2):157–179. https://doi.org/10.1016/j.resconrec.2007.06.007

Lavanya G (2015) and Josephraj Jegan. Durability Study on High Calcium Fly Ash Based Geopolymer Concrete. *Advances in Materials Science and Engineering* 2015. https://doi.org/10.1155/2015/731056

Mehta A, and Rafat Siddique (2017) Sulfuric acid resistance of fly Ash based Geopolymer concrete. Constr Build Mater 146:136–143. https://doi.org/10.1016/j.conbuildmat.2017.04.077

Milkey RG (1960) Infrared Spectra of some tectosilicates. Am Mineral 45(September–October):990–1007

Mohammed AA, Ahmed HU, and Amir Mosavi (2021) Survey of Mechanical properties of Geopolymer concrete: a Comprehensive Review and Data Analysis. Materials 14(16). https://doi.org/10.3390/ma14164690

Mustafa M, Bakri A, Mohammed H, Kamarudin H, Khairul Niza I, Zarina Y (2011) Review on fly Ash-based Geopolymer concrete without Portland Cement. J Eng Technol Res 3(1):1–4

Nath P, and Prabir Kumar Sarker (2014) Effect of GGBFS on setting, Workability and Early Strength properties of fly Ash Geopolymer concrete cured in Ambient Condition. Constr Build Mater 66:163–171. https://doi.org/10.1016/j.conbuildmat.2014.05.080

Nath P, and Prabir Kumar Sarker (2017) Flexural Strength and Elastic Modulus of ambient-cured blended low-calcium fly Ash Geopolymer concrete. Constr Build Mater 130:22–31. https://doi.org/10.1016/j.conbuildmat.2016.11.034

Naveen Kumar D, Ramujee K (2017) *ABRASION RESISTANCE OF POLYPROPYLENE FIBER REINFORCED GEOPOLYMER CONCRETE*. Vol. 4

Oyebisi S, Ede A, Olutoge F, Omole D (2020) Geopolymer concrete incorporating Agro-industrial Wastes: effects on Mechanical Properties, Microstructural Behaviour and Mineralogical Phases. Constr Build Mater 256:119390. https://doi.org/10.1016/j.conbuildmat.2020.119390

Park SM, Jang JG, Lee NK, Lee HK (2016) Physicochemical Properties of Binder Gel in Alkali-Activated Fly Ash/Slag exposed to high temperatures. Cem Concr Res 89:72–79. https://doi.org/10.1016/j.cemconres.2016.08.004

Phair JW, Van Deventer JSJ, Smith JD (2000) Mechanism of Polysialation in the incorporation of Zirconia into fly Ash-based geopolymers. Ind Eng Chem Res 39(8):2925–2934. https://doi.org/10.1021/ie990929w

Puligilla S, and Paramita Mondal (2013) Role of Slag in Microstructural Development and Hardening of fly Ash-Slag Geopolymer. Cem Concr Res 43:70–80. https://doi.org/10.1016/j.cemconres.2012.10.004

Raymond H, Myers DC, Montgomery CM, Anderson-Cook (2016) Response Surface Methodology: Process and Product Optimization Using Designed Experiments. *Wiley*

Sethi H, Bansal PP, and Raju Sharma (2019) Effect of Addition of GGBS and Glass Powder on the properties of Geopolymer concrete. Iran J Sci Technol Trans Civil Eng 43(4):607–617. https://doi.org/10.1007/s40996-018-0202-4

Singh A, Bhadauria SS, Thakare AA, Kumar A, Mudgal M, and Sandeep Chaudhary (2024) Durability Assessment of Mechanochemically activated Geopolymer concrete with a low Molarity Alkali Solution. Case Stud Constr Mater 20. https://doi.org/10.1016/j.cscm.2023.e02715

Standard ASTM (2018) ASTM C33/C33M–18 standard specification for concrete aggregates. West Conshohocken, PA

Sunagar P, Mahesh C, Kumar L, Shwetha K, G, and Kiran B. M (2021) Strength and durability behaviour of fly Ash based Geopolymer concrete in Structural Applications. Nat Volatiles Essent Oils 8(4):3088–3100

Tanu HM (2022) and Sujatha Unnikrishnan. Utilization of Industrial and Agricultural Waste Materials for the Development of Geopolymer Concrete- A Review. *Materials Today: Proceedings* 65:1290–97. https://doi.org/10.1016/j.matpr.2022.04.192

Tanu HM (2023) and Sujatha Unnikrishnan. Review on Durability of Geopolymer Concrete Developed with Industrial and Agricultural Byproducts. *Materials Today: Proceedings*. https://doi.org/10.1016/j.matpr.2023.03.335

Thokchom S, Ghosh P, and Somnath Ghosh (2009) Effect of water absorption, Porosity and sorptivity on durability of Geopolymer Mortars. J Eng Appl Sci 4(7):28–32

Tushar D, Das D, Pani A, and Pratyasha Singh (2022) Geo-Engineering and Microstructural Properties of Geopolymer Concrete and Motar: a review. Iran J Sci Technol - Trans Civil Eng 46(4):2713–2737. https://doi.org/10.1007/s40996-021-00756-y

van Deventer JSJ, Provis JL, Duxson P, Lukey GC (2007) Reaction mechanisms in the Geopolymeric Conversion of Inorganic Waste to useful products. J Hazard Mater 139(3):506–513. https://doi.org/10.1016/j.jhazmat.2006.02.044

Wang A, Zheng Y, Zhang Z, Liu K, Li Y, Shi L, and Daosheng Sun (2020) The durability of Alkali-activated materials in comparison with ordinary Portland Cements and concretes: a review. Engineering 6(6):695–706. https://doi.org/10.1016/j.eng.2019.08.019

Xu H, Van Deventer JSJ (2000) The geopolymerisation of Alumino-Silicate minerals. Int J Miner Process 59(3):247–266. https://doi.org/10.1016/S0301-7516(99)00074-5

Yunsheng Z, Wei S, Qianli C, and Chen Lin (2007) Synthesis and heavy metal immobilization behaviors of Slag based Geopolymer. J Hazard Mater 143(1–2):206–213. https://doi.org/10.1016/j.jhazmat.2006.09.033

Zhang B (2024) Durability of low-Carbon Geopolymer concrete: a critical review. Sustainable Mater Technol 40:e00882. https://doi.org/10.1016/j.susmat.2024.e00882